

HEAT TRANSFER AND FLUID FLOW SIMULATION IN A CLOSED-LOOP NATURAL CIRCULATION SOLAR WATER HEATING SYSTEM

Leandro da Silva Sales

Departamento de Mecânica, UNIFEI, Itajubá, MG, Brazil
leandro8746@hotmail.com

Ricardo Dias Martins de Carvalho

Departamento de Mecânica, UNIFEI, Itajubá, MG, Brazil
martins@iem.efei.br

Abstract. *In this work, a computer routine was written to simulate the operation of a natural circulation, domestic water heating system. Basically, the system was made of the flat-plate collectors, storage tank, and connecting piping. This was considered to be more representative of domestic solar water heaters used in Brazil. The routine was then used to assess the influence of several design parameters on the system performance and come up with an improved design. Next, the operation of the improved design system was simulated assuming it was located in Itajubá, MG, southeast Brazil. Raw weather data for Itajubá collected by the Brazilian National Space Research Institute (INPE) were reduced for use in the simulation.*

Keywords. *Solar water heater, natural circulation, computer simulation*

1. Introduction

Approximately 21% of the electric energy supply to residential consumers in Brazil is used for heating water in electric showers. In this connection, solar water heaters represent an excellent alternative that can substantially reduce the electric energy peak demand. Since water temperatures in the 30 to 40°C range is already appropriate for shower and kitchen use, the solar heater could be built from less expensive materials indicated for moderate temperatures. In addition, costs could be further reduced if the solar heater is of the natural circulation type. In this investigation a complete natural circulation solar water heating system (solar collector, storage tank, and connecting pipes) was modeled. Operation of the systems modeled was simulated assuming they were located in Itajubá (45:27W, 22:26S, 840 m elevation), Minas Gerais State, southeast Brazil. It was then possible to determine the expected system performance for each month of the year.

2. Determination of the Thermosyphon Flow Rate and the Heat Transfer Coefficient in the Collector Tubes

Briefly, a typical flat-plate solar collector is comprised of the solar energy absorbing surface, tubes through which flows the fluid receiving the absorbed energy, a transparent cover over the absorbing surface which reduces convection and radiation losses to the atmosphere, and back insulation to reduce conduction losses. In the case of solar water heaters with natural circulation the flow conditions inside the tubes are directly dependent on the amount of solar energy absorbed and the system layout. In this section a mathematical model is discussed that allowed for the determination of the thermosyphon mass flow rate and the heat transfer coefficient in the collector tubes. As the model will eventually be used to assess the performance of commercially available solar water heaters, the input required should pertain only to the system geometry and constructive materials, and weather data (solar radiation influx, ambient air temperature, and wind velocity). Based on these criteria, the model by Gupta and Garg (1968) was deemed an appropriate starting point for the present work.

Gupta and Garg (1968) modified the basic model due to Close (1962) so as to take into account the system thermal capacity and the heat exchanger efficiency of the collector. Referring to Figure 1, the main assumptions in their model, which were also retained in the present investigation, are: (1) There is no hot water drain-off during the day; (2) The mean water temperature in the tank is the same as the mean water temperature in the collector during sun up hours (approximately, from 9:30 a.m. to 2:30 p.m.); (3) The mean water temperature in the connecting pipes is also equal to the mean water temperature in the tank when both the discharge and return pipes are considered; (4) In view of the fairly large temperature range over which the system operates throughout the day, the relationship between the water specific gravity and temperature is better represented by a quadratic function, $SG = aT^2 + bT + c$; (5) For purposes of calculating the thermal capacities of the system components throughout the day, the temperature of these same components can be made equal to the temperature of the water in them.

An instantaneous energy balance applied to the collector and pipes leads to (nomenclature in Table 2)

$$\dot{m}_p (T_3 - T_5) = F_R A_c [H_t (\tau\alpha)_e - U_c (T_m - T_a)] - \left(C_{cw} \frac{dT_p}{d\theta} \right) - \left(C_{cpw} \frac{dT_{cp}}{d\theta} \right) - U_{cp} (T_{w,cp} - T_a) \quad (1)$$

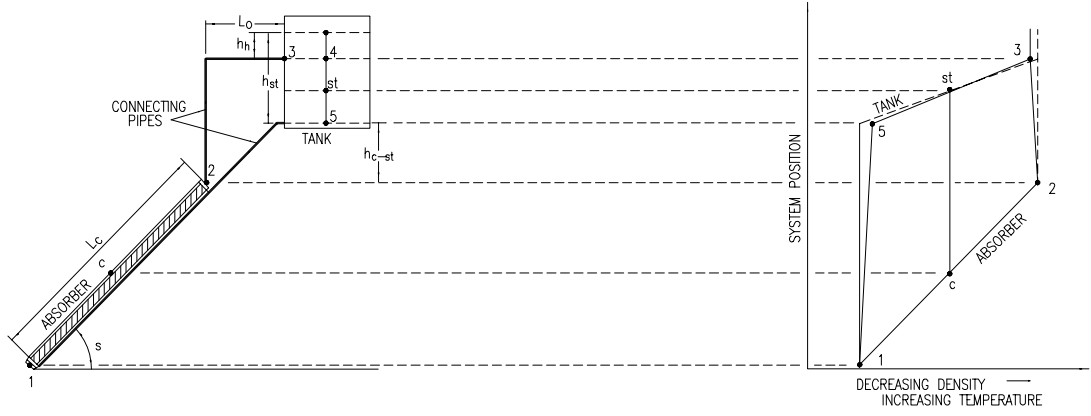


Figure 1: Solar water heater layout and corresponding density distribution diagram.

The thermal pressure head generated by solar heating, i. e. the area of the density distribution diagram (Figure 1), is given by Eq. (2), below, where $f(h)$ is the system function determined in terms of the pipes layout, height of water in the tank, and collector length and tilt, Eq. (3). In Eq. (2) a and b are the coefficients of the equation $SG = aT^2 + bT + c$.

$$p_w = \frac{T_5 - T_3}{2} (2aT_m + b)f(h) \quad (2)$$

$$f(h) = [L_c \sin(s) + 2h_{c-st} + (h_{st} - h_h)] \quad (3)$$

On the other hand, an energy balance applied to the storage tank reduces to

$$\dot{m}c_p(T_3 - T_5) = C_{st} \frac{dT_{st}}{d\theta} + U_r(T_{st} - T_a) \quad (4)$$

where, according to assumption (2) above, $T_{st} = (T_2 + T_1)/2$. Now, the thermosyphon flow rate will be such that at any instant the thermal pressure head is balanced by the frictional head loss in the flow circuit. Combining Eqs. (2) and (4) and introducing Darcy-Weisbach's equation for the frictional head loss, one finally gets the thermosyphon flow equation

$$\dot{m}^3 = -\frac{\pi^2 \rho^2 g (d_{i,cp})^5}{16f L_{loop} c_p} \left[C_{st} \frac{dT_{st}}{d\theta} + U_{st}(T_{st} - T_a) \right] (2aT_{st} + b)f(h) \quad (5)$$

where

$$L_{loop} = \left[\frac{WL_c}{L_h} \left(\frac{d_{i,cp}}{d_{i,r}} \right)^5 + L_h \left(\frac{d_{i,cp}}{d_{i,h}} \right)^5 \right] + [L_c + H_{st} - h_h + h_{c-st}(1 + \cos ec(s))] + L_m + L_o \quad (6)$$

Ouzzane and Galanis (2001) numerically studied the laminar mixed convection in the entrance region of an inclined tube with longitudinal external fins, a geometry corresponding to the basic element of flat plate solar collectors. Their results showed that the heat transfer inside the tubes is considerably higher for the finned tube than that for the bare tube. Baker (1967) conducted an experimental investigation on the heat transfer in solar collector tubes at low Reynolds numbers. He concluded that, due to significant variations in the circumferential wall temperature, the heat transfer rates are higher than those obtained in a tube with uniform wall temperature. In addition, mixed convection is most likely to occur under these conditions and the correlations by Oliver (1962) were thought to provide a reliable means for the determination of the heat transfer coefficient. Based on these arguments, Kazeminejad (2002) decided for its use in his investigation of the fluid flow in flat-plate solar collectors. It is felt that their use in the present work is also warranted.

$$Nu_m = 1.75 \left(\frac{\mu_b}{\mu_w} \right)^{0.14} \left[Gz_m + 0.0083 (Gr_m Pr_m)^{0.75} \right]^{\frac{1}{3}} \quad \text{for } L/d_i \text{ ratio} > 70 \quad (7)$$

$$Nu_m = 1.75 \left(\frac{\mu_b}{\mu_w} \right)^{0.14} \left[Gz_m + 0.00056 \left(Gr_m Pr_m \frac{L_r}{d_i} \right)^{0.70} \right]^{\frac{1}{3}} \quad \text{for } L/d_i \text{ ratio} < 70 \quad (8)$$

3. Meteorological Data for Itajubá

The Brazilian *National Space Research Institute* (INPE) has a nationwide network of platforms for collecting climatic data for use in weather forecast models. One of these platforms is located in Itajubá and has been in service since April 1998. Of special interest to the present study, the following data are available: ambient air dry bulb temperature; wind velocity and direction 10 m above ground level; accumulated total solar radiation. Ideally, hourly profiles of the climatic variables should be available for the evaluation of solar processes' performance. However, due to limitations in the satellite transmission, data are collected every three hours only (0, 3, 6, 9, 12, 15, 18, and 21 GMT). Furthermore, the raw data as collected by INPE did not lend themselves for use in this investigation and had to be reduced so that they could be used in this simulation. A three-year-period data set was available (April 1998 through July 2001) when the data reduction routine was written and this constitutes the basis for this investigation. An upgrade of this routine using more sophisticated statistical methods and the now available larger data sets is planned for the near future and will be the object of another paper. The data collecting procedure used by INPE for each of the climatic variables above and their reduction by the present authors are discussed below.

The air-dry bulb temperature is measured by a platinum RTD, placed inside a protective porous casing to avoid damage by ambient dust and moisture. In addition, the assembly is sheltered from rain and direct exposure to sunshine by a plastic rain cap. The values reported by INPE are instantaneous readings of the air temperature in degrees Celsius collected every three hours. On the basis of the three-year-period data sample, the present authors calculated the monthly mean temperatures (see Table 1) and the monthly mean temperature profiles (*T x time of the day*). The reduced data were then used in the simulation to evaluate the heat losses from the collector, pipes, and storage tank.

The device for measuring wind velocity and direction is an ultrasonic sensor located 10m above ground level, which determines the wind velocity and direction on a horizontal plane. The data are collected every second over a 10-min period preceding the reported hour of measurement. In other words, the readings reported by INPE are in fact mean values of 600 data points collected every three hours. The wind velocity is given in *m/sec* and the wind direction in degrees measured clockwise from the actual North. From the three-year data sample, the present authors calculated the monthly mean wind velocities (Table 1) and the hourly mean velocities for each month of the year (values available every three hours only). These wind velocities were then used in the simulation to evaluate the convection heat transfer coefficient over the collector glass cover. In these calculations, no consideration was made of the wind direction.

The device for measuring the radiation flux generates an electric current proportional to the intensity of the total (beam plus diffuse) solar radiation received from the hemisphere centered above a horizontal, semiconductor sensor. The data reported refer to the accumulated radiation in MJ/m^2 over three-hour intervals. This means the measuring device is reset every three hours.

In this investigation, these raw data were reduced so as to obtain the daily-accumulated radiation for each day in the data sample. Next, mean values of the daily-accumulated radiation for each month of the year were calculated (Table 1). However, in order to assess the natural circulation solar heater performance throughout the day, hourly profiles of the accumulated radiation were still necessary. The *Radiasol* computer routine (RADIASOL, 2002) was then used to obtain these profiles from the monthly mean values of the daily-accumulated radiation. This routine also allows for calculation of the radiation fluxes on a tilted surface from the data for the horizontal surface. It can be seen that the 33° collector tilt (latitude + 10°) maximizes the radiation flux on the collector during the winter months.

Table 1: Year round profile of climatic variables in Itajubá.

Month	T_{month} [°C]	V_{month} [m/sec]	H [kJ/m ² .day]	H_t [kJ/m ² .day]
Jan.	22.5	3.0	19730	17898
Feb.	22.3	3.0	18870	17748
Mar.	21.7	2.9	17880	17990
Apr.	19.7	3.0	18910	22038
May	15.9	2.4	14940	18910
Jun.	16.1	2.8	13440	17970
Jul.	15.3	2.2	14380	19554
Aug.	16.7	2.5	16770	20440
Sept.	18.8	2.6	17530	18572
Oct.	20.6	2.8	18880	18222
Nov.	20.6	2.7	19770	18080
Dec.	22.0	3.7	18790	17044

4. System Performance Calculation Procedure

The main steps of the calculation procedure implemented on the computer routine are given below. Where needed, the physical properties of air as a function of temperature were programmed using the relations by Rankine and Charters (1969).

1. Once the reduced weather data were available, the parameters calculated next were the heat transfer coefficient due to wind on the collector cover and the overall heat transfer coefficients through the collector cover and edges.
2. An iterative procedure then allowed for the calculation of the overall heat transfer coefficient through the collector top, the thermosyphon water flow rate, and the mean storage tank water temperature. In this procedure, the model for the complete solar system by Gupta and Garg (1968), the correlations by Oliver (1962), and the model for the collector itself by Duffie and Beckman (1974) were used. The convection heat transfer coefficient in the rectangular confined space between the absorbing plate and the glass cover was obtained using the correlation by Hollands *et al.* (1976), which made calculations somewhat more straightforward.
3. From the hourly values of the mean flow rate and the accumulated energy in the storage tank obtained above, the daily mean flow rate and the mean storage tank water temperature at the end of the day were calculated.

Before using the computer routine to evaluate the performance of solar water heaters in Itajubá, which is the main objective of this investigation, a comparison was made between available experimental data in the literature (Kalogirou and Papamarcou, 2000; Gupta and Garg (1968); Shitzer *et al.*, 1979; Huang and Hsieh, 1985; Nahar, 2002; Nahar, 2003) and numerical results from the routine for the same system geometry and weather conditions. The comparison was made on the basis of the daily variation of the storage tank mean water temperature. As can be seen in Figure 2, the numerical results agree with the experimental data within $\pm 4^{\circ}\text{C}$ except for the data from Nahar (2003), in which case the discrepancy can be as high as 10°C . However, the numerical results for comparison with the data from Nahar (2003) were obtained using reported daily average conditions instead of hourly profiles, as was done for the other authors. In addition, some physical properties and geometrical parameters were not reported and had to be assumed in this work. In view of these considerations, the present authors concluded for the soundness and reliability of the computer routine.

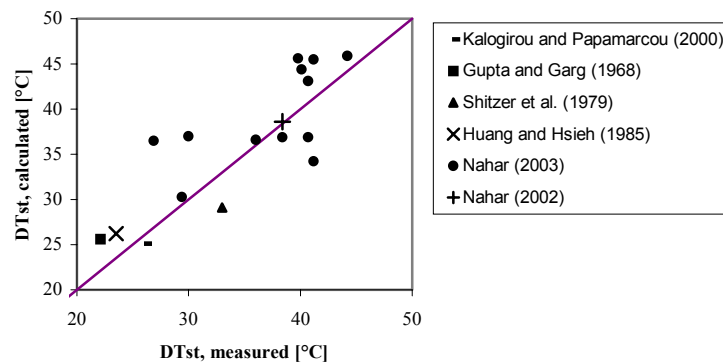


Figure 2: Daily increase in the storage tank water temperature, numerical results versus experimental values in the literature.

5. Numerical Results and Analysis

Solar System Design Optimization: In order to establish the influence of the main design parameters on the performance of solar water heaters, the design by Kalogirou and Papamarcou (2000) was taken as a starting point (Table 2). The following design parameters were then varied: number and diameter of collector tubes (risers); diameter of connecting pipes; storage tank insulation thickness; collector back insulation thickness; vertical distance between the collector top header and the cold water outlet in the tank bottom. Figure 3 and Figure 4 show the effect of the total number of collector tubes on, respectively, the daily mean thermosyphon flow rate and the storage tank mean water temperature at the end of the day. It can be seen that both the flow rate and the tank water temperature increase rapidly as the number of tubes is increased up to about 16 and then remain essentially constant thereafter. This is due to the increase in the fin efficiency, F , when the number of tubes is first augmented. However, as the number of tubes is further increased the fin efficiency starts dropping and the *useful energy gain per tube \times total number of tubes* product remains essentially constant. It was concluded that 16 risers (eight risers per plate) are quite satisfactory for this application.

Figure 5 and Figure 6 show the effect of the collector tubes diameter on the flow rate and storage tank mean water temperature, respectively. It can be observed that the flow rate increases rapidly as the tubes diameter is increased up to about 14 mm and then remains essentially constant. This is probably due to an initial enhancement in heat transfer to water associated with higher flow rates, as the friction loss decreases rapidly in the beginning. However, as the diameter gets larger the reduction in friction loss is no longer accompanied by a corresponding increase in heat transfer; actually, the heat transfer could even deteriorate due to decreased flow velocities. These opposing effects would then cancel each other out and the flow rate remains virtually constant. As long as there is an increase in both the flow rate and heat transfer, the useful energy gain increases rapidly and so does the storage tank mean water temperature at the end of the day. Once the flow rate levels off and heat transfer in the tubes degrades, the absorber plate temperature tends to increase, causing an increase in the collector losses. The net result is a reduction in the accumulated energy gain with a

consequent drop in the tank mean water temperature. For this particular case, the optimum corresponds to 11-mm-diameter-tubes. The conclusion can then be drawn that ten to twelve 11-mm-diameter tubes seem most appropriate for this particular application.

Table 2: Solar water heater designs.

	Kalogirou and Papamarcou (2000)	Improved Kalogirou and Papamarcou Design	Low Cost Design
General Features			
Number of collector plates	2	2	2
Number of risers per plate	12	8	8
Risers material	Copper	Copper	Galvanized Steel
Risers thermal conductivity, k [W/m.K]	385	385	205
Risers specific heat, c_p [J/kg.K]	385	385	903
Risers density, ρ [kg/m ³]	8,933	8,933	2,702
Risers $d_{i,r}/d_{o,r}$ [mm]	13.5 x 15	11.0 x 12.0	11.0 x 12.0
Absorber plate dimensions [m x m]	1.42 x 0.95	1.42 x 0.95	1.42 x 0.95
Overall dimensions [m x m x m]	1.42 x 1.9 x 0.078	1.42 x 1.9 x 0.098	1.42 x 1.9 x 0.098
Air gap between absorber and cover [cm]	1.6	1.6	1.6
Collector tilt from horizontal, s [°]	33	33	33
Collector top - tank base height, h_{c-st} [m]	0	0.5	0.5
Water height above storage tank inlet, h_h [m]	0.334	0.334	0.334
Water height above storage tank outlet, h_{st} [m]	0.564	0.564	0.564
Collector top - tank horizontal distance, L_o [m]	0.230	0.230	0.230
Collector Insulation			
Material	Fiberglass	Fiberglass	Fiberglass
Thermal conductivity, k [W/m.K]	0.038	0.038	0.038
Specific heat, c_p [J/kg.K]	835	835	835
Density, ρ [kg/m ³]	32	32	32
Back insulation thickness [cm]	5	7	7
Edges insulation thickness [cm]	3	3	3
Absorbing Plate			
Material	Copper	Copper	Aluminum
Thickness, t [mm]	1	1	1
Black paint emissivity, ε	0.94	0.94	0.94
Black paint absorptivity, α	0.90	0.90	0.90
Transparent Cover			
Material	Glass	Glass	Glass
Thickness, t [mm]	4	4	4
Number of covers	1	1	1
Specific heat, c_p [J/kg.K]	750	750	750
Density, ρ [kg/m ³]	2,500	2,500	2,500
Emissivity, ε	0.90	0.90	0.90
Transmissivity, τ	0.80	0.80	0.80
Refraction index, n	1.526	1.526	1.526
Connecting Pipes			
Material	Copper	Copper	Galvanized Steel
Length, L_{cp} [m]	2.39	2.39	2.39
$d_{i,cp}/d_{o,cp}$ [mm]	20.0 x 22.0	20.0 x 22.0	20.0 x 22.0
Number of bends	4	4	4
Insulation material	Polyurethane	Polyurethane	Polyurethane
Insulation thickness, t [cm]	0.5	0.5	0.5
Insulation thermal conductivity, k [W/m.K]	0.038	0.038	0.038
Hot Water Storage Tank			
Volume [liters]	150	150	150
Length, L_{st} [cm]	60	60	60
$d_{i,st}/d_{o,st}$ [cm]	56.4 / 68.4	56.4 / 68.4	56.4 / 68.4
Insulation material	Polyurethane	Polyurethane	Polyurethane
Insulation thickness, t [cm]	6	6	6

Note: The parameters changed from one design to the next are typed in boldface.

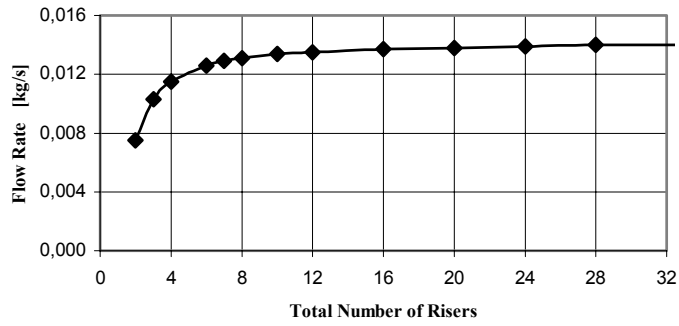


Figure 3: Thermosyphon flow rate as a function of the total number of collector risers.

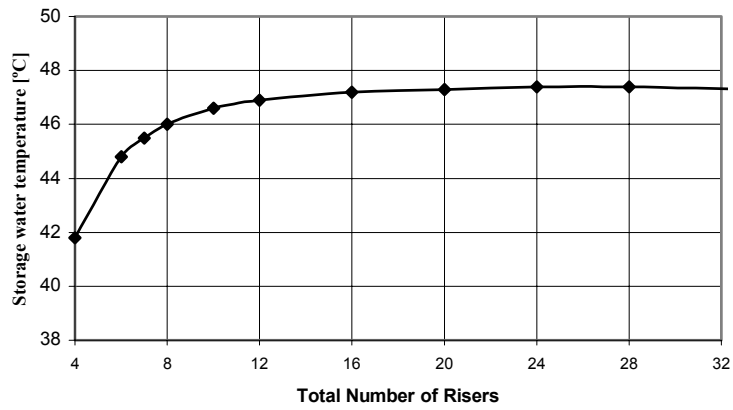


Figure 4: Storage tank mean water temperature as a function of the total number of collector risers.

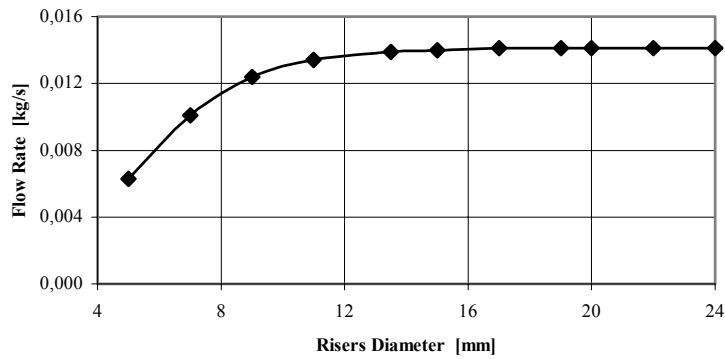


Figure 5: Thermosyphon flow rate as a function of the collector risers diameter.

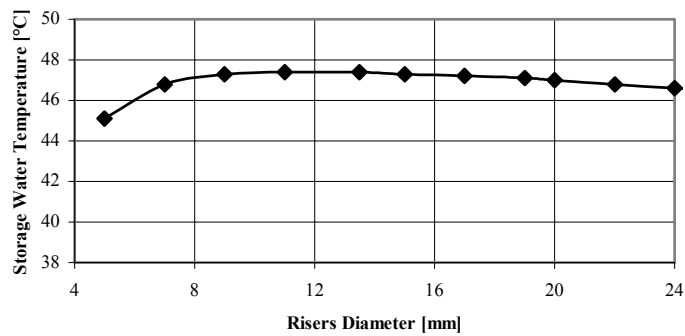


Figure 6: Storage tank mean water temperature as a function of the collector risers diameter.

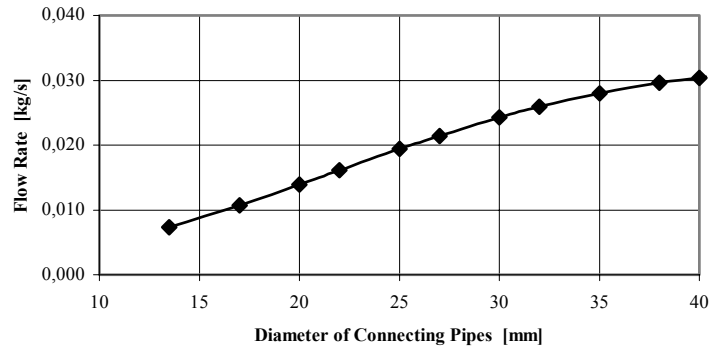


Figure 7: Thermosyphon flow rate as a function of the connecting pipes diameter.

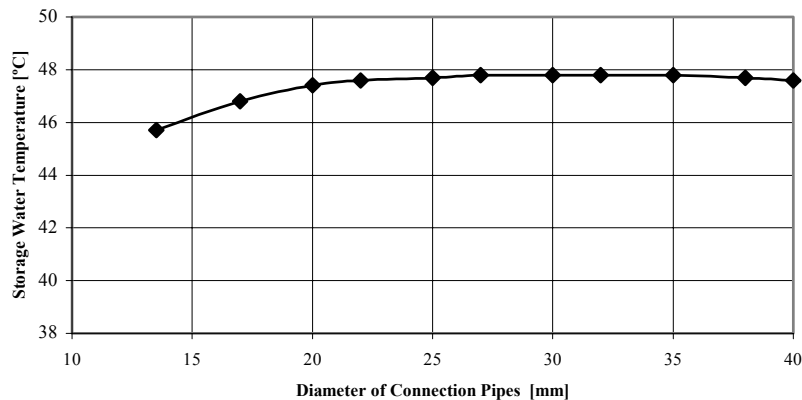


Figure 8: Storage tank mean water temperature as a function of the connecting pipes diameter.

Figure 7 and Figure 8 show the effect of the connecting pipes diameter on, respectively, the daily mean flow rate and the storage tank mean water temperature. As one would expect, an increase in the pipes diameter leads to an increase in the flow rate due to the reduction in the friction loss. The tank water temperature increases rapidly in the beginning and then levels off for 22-mm-diameter pipes and larger. This could be related to increasingly larger circulation times as the flow velocities in the connecting pipes decreases. In the other words, the accumulated energy gain is not substantially increased once the circulation times get too long. Apparently, 22-mm-diameter pipes are a reasonable choice for this application.

Modifications based on these trends were made to the design by Kalogirou and Papamarcou (2000) (Table 2). The modifications were only minor as the original design was already close to optimum. Next, this modified design was once again changed so that the influence of alternate materials on the system performance could be checked. Nahar (2002) conducted a long-term study of solar water heaters built with alternate materials to reduce costs. Instead of copper, the collector tubes were made of galvanized steel and the absorbing plate was made of aluminum. In Table 2, the column named *low cost design* reflects these and other modifications following the design by Nahar (2002). (Once again, the parameters changed are typed in boldface.)

Figure 9 and Figure 10 show the storage tank mean water temperature at the end of the day as a function of, respectively, the collector back insulation thickness and the storage tank insulation thickness. The water temperature increase when the collector insulation thickness is increased from 5 cm (the thickness actually used by Kalogirou, and Papamarcou (2000) to 7 cm is 1°C; this was the value used in the improved design. Regarding the storage tank insulation, it can be seen that a mere 0.5°C is gained when the insulation thickness is increased from 6 cm to 10 cm. Therefore, it was kept at the original 6-cm value.

Figure 11 and Figure 12 show the effect of the vertical distance between the storage tank cold water outlet and the collector top header on, respectively, the thermosyphon flow rate and the tank mean water temperature at the end of the day. The negative values for h_{c-st} indicate that the collector top level is higher than the tank bottom. Due to the increased pressure head, there is a significant, continuous increase in the flow rate when h_{c-st} is increased. On the other hand, the four-fold increase in h_{c-st} causes the tank water temperature to increase less than 1.5°C. It is then concluded that the design value for h_{c-st} should take into account primarily the specific layout restrictions of the application at hand, the system thermal performance hardly being affected by it. Hence, in this investigation the 0.30 to 0.70 m rule-of-thumb was applied and h_{c-st} was taken as 0.50 m.

Performance of Solar Systems in Itajubá: Figure 13 shows the solar systems efficiencies for each month of the year. Due to lack of data, the initial water inlet temperature, as circulation starts in the morning, was assumed equal to the air temperature. The general trends are as expected, that is, higher efficiencies during the winter months, which are a direct consequence of the higher useful heat gains at this time of the year. One should remember that lower water inlet temperatures in winter lead to greater temperature differences between the absorber plate and the water. Next, it is observed that there is no significant difference between the Kalogirou and Papamarcou (2000) design and the Kalogirou and Papamarcou improved design. This result testifies to the soundness of the authors' original design. Regarding the efficiency of the low cost design, it is systematically lower than the other two even though the difference is minimal (approximately 0.6%). These lower efficiencies are most likely due to greater heat losses related to the use of less expensive materials.

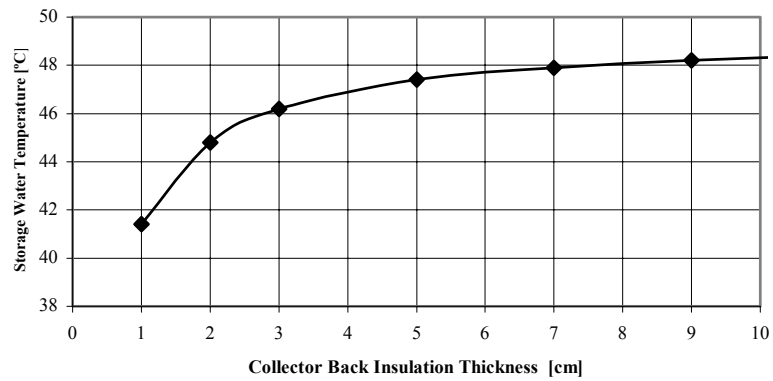


Figure 9: Storage tank mean water temperature as a function of the collector back insulation thickness.

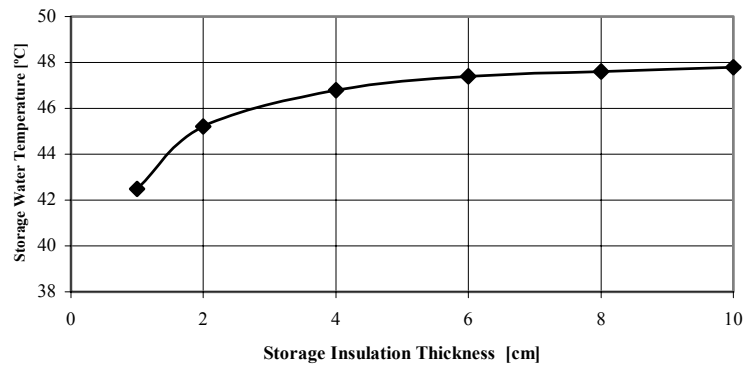


Figure 10: Storage tank mean water temperature as a function of the tank insulation thickness.

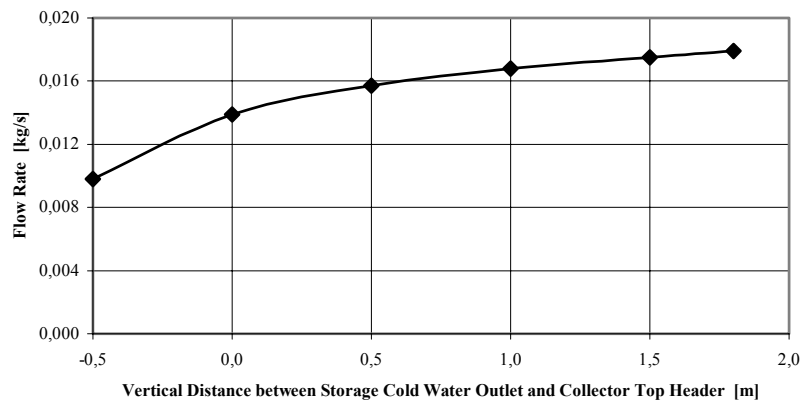


Figure 11: Thermosyphon flow rate as a function of the vertical distance between the storage tank cold water outlet and the collector top header.

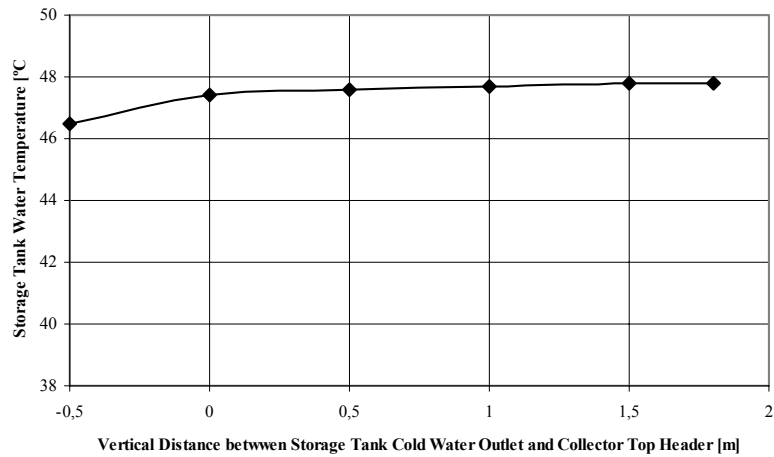


Figure 12: Storage tank mean water temperature as a function of the vertical distance between the storage tank cold water outlet and the collector top header.

Finally, Figure 14 shows the storage tank water temperature at the end of the day for each month of the year. Once again, during the winter months lower temperatures occur due to greater heat losses to the colder ambient air. Surprisingly, the low cost design leads to systematically higher temperatures all year round however minimal the difference (approximately 0.5°C). These trends agree with those observed by Nahar (2002) who concluded that this behavior is due to the fact that the thermal conductances of the aluminum plate and the copper plate are almost the same (0.0979 and 0.0974 WK⁻¹, respectively). Even though the thermal conductivity of aluminum ($k = 205 \text{ Wm}^{-1}\text{K}^{-1}$) is less than that of copper ($k = 385 \text{ Wm}^{-1}\text{K}^{-1}$), the aluminum plate is thicker than the copper one (0.4775 mm and 0.2591 mm, respectively) as used by manufacturers. In connection with the rather low temperatures for months like November and December, one should bear in mind that the collector tilt maximizes the radiation flux on the collector during the winter months and reduces it during warmer months. Whatever the case, all temperatures are within the 43 to 47°C range, therefore appropriate for showers and kitchen use. The substantially larger result for the month of April seems to be due to a problem with the original radiation data.

6. Conclusions

The design and operation of natural circulation solar water heaters have been studied. The systems were supposed located in Itajubá, Minas Gerais State, southeast Brazil. Following are the main conclusions:

1. The design by Kalogirou and Papamarcou (2000) was optimized using the computer routine developed in this work. Details of this design and the ones derived from it can be seen in Table 2.
2. The *low cost design* using alternate materials as suggested by Nahar (2002) performed just as well.
3. The water temperatures at the end of the day for any design were within the 43 to 47°C range, therefore appropriate for showers and kitchen use.

Further studies of solar water heaters are planned for the near future. In particular, the low cost system will be built and tested and a detailed cost-performance analysis will be made. In addition, an upgrade of the routine for reducing meteorological data is also planned and will be applied to the now larger weather data samples.

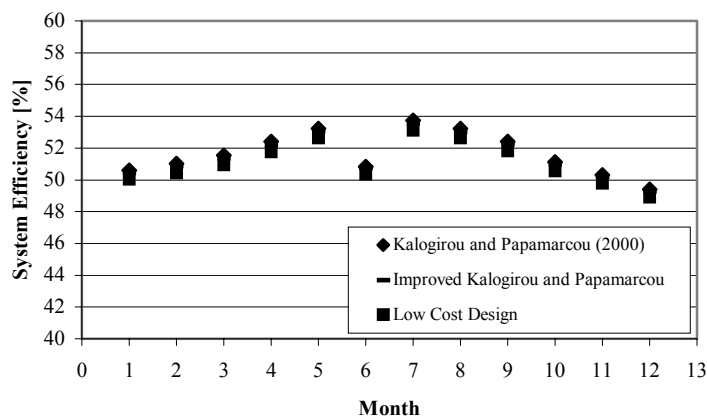


Figure 13: Solar systems efficiencies throughout the year in Itajubá.

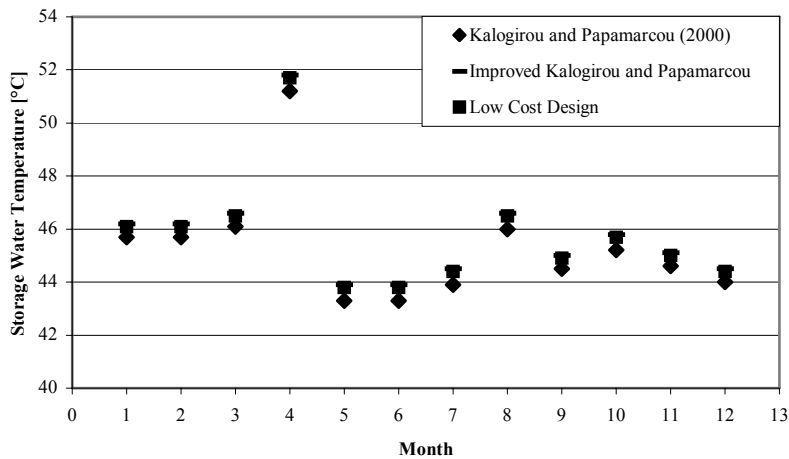


Figure 14: Storage tank water temperature at the end of the day throughout the year in Itajubá.

7. Acknowledgement

The authors are grateful to Mr. Flávio de Carvalho Magina from the Brazilian *National Space Research Institute* (INPE) for providing the meteorological data for this study.

8. References

- Baker, L. H., 1967, "Film Heat-Transfer Coefficients in Solar Collector Tubes at Low Reynolds Numbers", *Solar Energy*, Vol. 11, pp. 78-85.
- Close, D. J., 1962, "The Performance of Solar Water Heaters with Natural Circulation", *Solar Energy*, Vol.6, pp. 33-40.
- Duffie, J. A. and Beckman, W. A., 1974, "Solar Energy Thermal Processes", John Wiley & Sons.
- Gupta, C. L. and Garg, H. P., 1968, "System Design in Solar Heaters with Natural Circulation", *Solar Energy*, Vol. 12, pp. 163-182.
- Hollands, K. G. T., Unny, S. E., Raithby, G. D. and Konicek, L., 1976, "Free Convective Heat Transfer across Inclined Air Layers", *Journal of Heat Transfer*, Vol. 98, pp 189.
- Huang, B. J. and Hsieh, C. T., 1985, "A Simulation Method for Solar Thermosyphon Collector", *Solar Energy*, Vol. 35, pp. 31-43.
- Kalogirou, S. A. and Papamarcou, C., 2000, "Modelling of a Thermosyphon Solar Water Heating System and Simple Model Validation", *Renewable Energy*, Vol. 21, pp. 471-493.
- Kazeminejad, H., 2002, "Numerical Analysis of Two-Dimensional Parallel Flow Flat-Plate Solar Collector", *Renewable Energy*, Vol. 26, pp. 309-323.
- Nahar, N. M., 2002, "Capital Cost and Economic Viability of Thermosyphonic Solar Water Heaters Manufactured from Alternate Materials in India", *Renewable Energy*, Vol. 26, pp. 623-635.
- Nahar, N. M., 2003, "Year Round Performance and Potential of a Natural Circulation Type of Solar Water Heater in India", *Energy and Buildings*, Vol. 35, pp. 239-247.
- Oliver, D. R., 1962, "The Effect of Natural Convection on Viscous Flow Heat Transfer in Horizontal Tubes", *Chemical Engineering Science*.
- Ouzzane, M. and Galanis, N., 2001, "Numerical Analysis of Mixed Convection in Inclined Tubes with External Longitudinal Fins", *Solar Energy*, Vol. 71, pp. 199-211.
- RADIASOL Computer Routine, 2002, Laboratório de Energia Solar, Grupo de Estudos Térmicos e Energéticos (GESTE), Universidade Federal do Rio Grande do Sul (UFRS), Brazil.
- Rankine, A. D. and Charters, W. W. S., 1969, "Combined Convective and Radiative Heat Losses from Flat – Plate Solar – Air Heaters", *Solar Energy*, Vol. 12, pp. 517-523.
- Shitzer, A., Kalmanoviz, D., Zvirin, Y., and Grossman, G., 1979, "Experiments with a Flat Plate Solar Water Heating System in Thermosyphonic Flow", *Solar Energy*, Vol. 22, pp. 27-35.